Synthesis and Structural Characterization of Ethynylene-Bridged Bisazines Featuring Various α-Substitution

Jörg Hübscher,[a] Wilhelm Seichter,[a] Thomas Gruber,[b] Jens Kortus,[b] and Edwin Weber[a]*

[a]Institut für Organische Chemie, Technische Universität Bergakademie Freiberg, Leipziger Strasse 29, D-09596 Freiberg, Germany
[b]Institut für Theoretische Physik, Technische Universität Bergakademie Freiberg, Leipziger Strasse 23, D-09596 Freiberg, Germany
*E-mail: edwin.weber@chemie.tu-freiberg.de

Received July 10, 2013
DOI 10.1002/jhet.2122
Published online 00 Month 2014 in Wiley Online Library (wileyonlinelibrary.com).

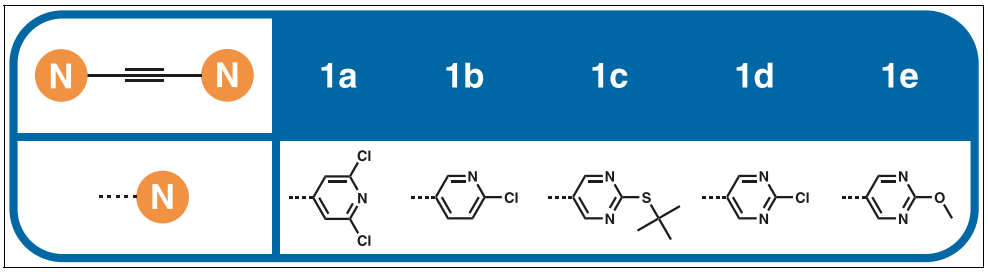

A series of bispyridines and bispyrimidines **1a–1e** showing the heterocycles attached to both ends of an ethynylene unit and being α-substituted with chloro, *tert*-butylthio, and methoxy groups have been synthesized *via* cross-coupling technique and their crystal structures studied by X-ray diffraction analysis. Supramolecular interactions of C–H···N and π···π stacking type were found to largely dominate the structures according to the compound species. A trial was given to deduce the markedly differing temperatures of melting among the compounds from special features of the crystal structures.

INTRODUCTION

Heterocycles have paved the way for a host of compounds being effective in different fields of application such as drugs [1–3], polymers [4], or complexants [5–7]. Considering the latter mode of application, linker molecules suitable for the construction of so-called coordination polymers or metal-organic framework structures based on aza heterocycles get increasingly to a center of interest [8,9]. In this respect, ethynylene-linked azines have been successfully used as linker molecules for the coordinative oligomerization [10,11] and polymerization [12–15] of appropriate metal ions. Moreover, in a sphere suited something different from before, respective molecules were also tested regarding the possibility to assist solid network formation *via* hydrogen bonding [16]. Among others, this has been realized with the formation of chain-linked capsules using intermolecular aggregation [17]. Following a related target, terminally functionalized analogues, in particular α-chlorinated ethynylene-bridged pyridines have proven to be key intermediates for the synthesis of conjugated tectones for supramolecular nanoengineering [18].

In the present article, we describe the synthesis of five linker-type azines composed of a central ethynylene moiety and terminal pyridine and pyrimidine units featuring different linkage modes (**1a**, **1b**) as well as different kinds and numbers of additional substituents, that is, chlorine (**1a**, **1b**, **1d**), *tert*-butylthio (**1c**), or methoxy (**1e**) being either electron withdrawing or donating groups, respectively (Scheme 1). These compounds were found to show interesting solid state structures that are also reported and comparatively discussed here, considering specific effects of the structural characteristics of the molecules exercising an influence on the supramolecular interaction modes.

RESULTS AND DISCUSSION

Synthesis. Due to the basic structure of compounds **1a–1e**, all being azine-terminated ethynes, their syntheses follow a rather uniform preparative route starting from iodo-substituted azines **4a–4e** (Scheme 2). They suitably meet the requirements for an intended coupling with the ethyne moiety typical of the target compounds. These azines, in the run-up to the synthesis, were obtained, applying different procedures known from the literature, except for **4c** that has not been described before. Referring to these transformations, **4a** was directly iodinated using Schlosser's conditions [19] and isolated by fractional crystallization from dry ethanol, while **4b** was prepared in two steps from 2-hydroxypyridine *via* 5-iodo-2-hydroxypyridine (**5**) [20]. At this point, we advise to perform the reaction for **5** by adding the aqueous NaOCl solution dropwise during 2 h at 40°C instead of 0°C that gave an increase of the yield of 12% compared with the literature [18]. Subsequent chlorination of **5** with

© 2014 HeteroCorporation

Scheme 1

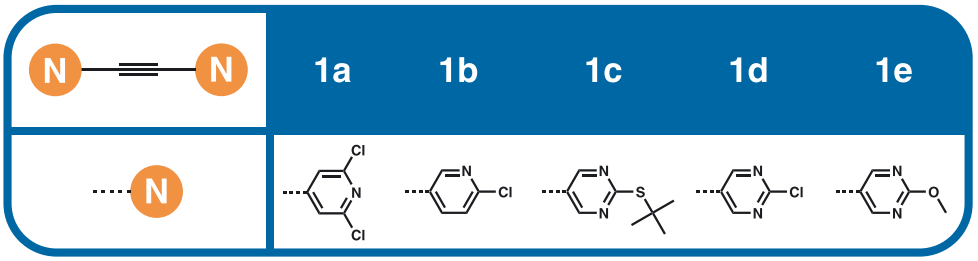

Scheme 2

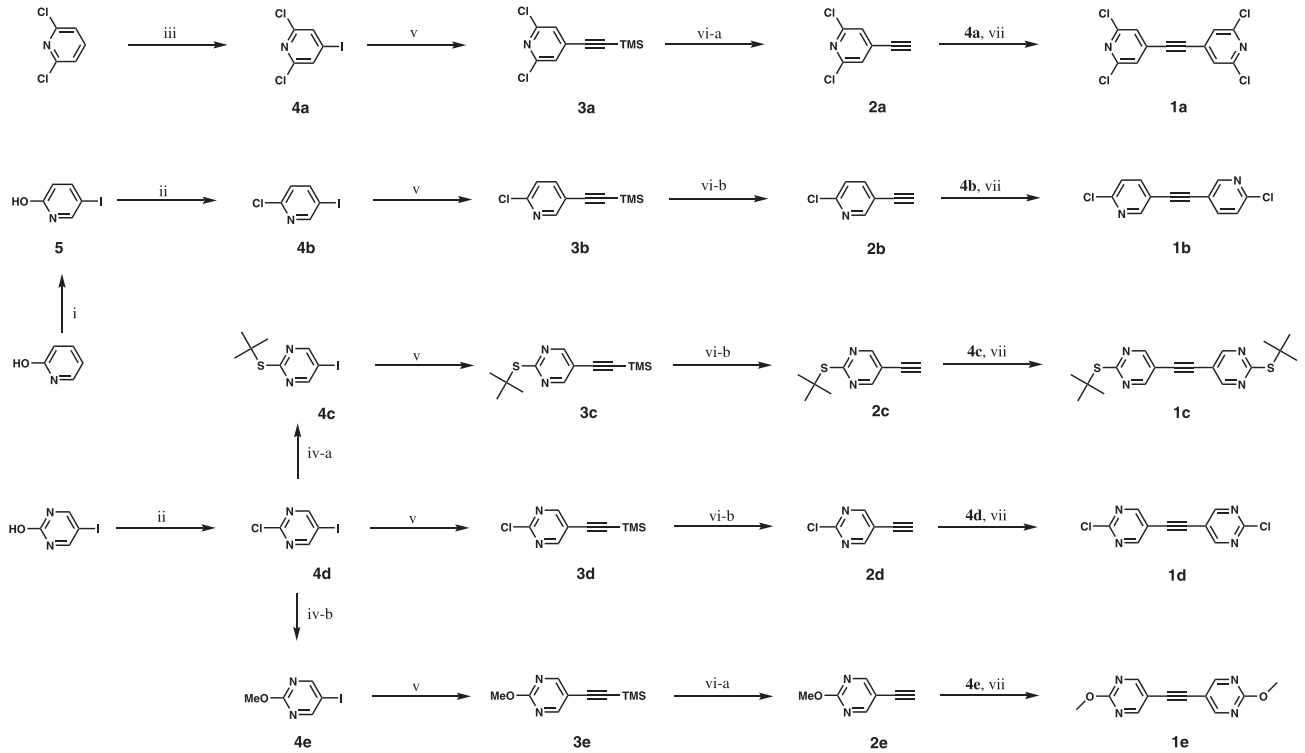

i) 1. NaI, NaOH, NaOCl; 2. HCl. ii) $POCl_3$, NET(i-Pr)$_2$, MeCN. iii) n-BuLi, I_2, THF. iv-a) t-BuSH, NaH, DMF. iv-b) NaOMe, MeOH. v) TMSA, $Pd(PPh_3)_2Cl_2$, PPh_3, CuI, DIPA, THF. vi-a) KOH, H_2O, MeOH, THF. vi-b) KOH, H_2O, MeCN. vii) $Pd(PPh_3)_2Cl_2$, PPh_3, CuI, DIPA, THF.

phosphorous oxychloride, successfully carried out by Schaetzer *et al.* [21], can also be performed in dry acetonitrile solution in the presence of Hünig's base to gain **4b** effortless in good yield according to our finding. By using the same chlorination method, **4d** was synthesized from 5-iodo-2-hydroxypyrimidine [22], which, at the same time, is also the precursor compound for the preparation of **4c** and **4e** obtained from nucleophilic substitution with sodium 2-methylpropane-2-thiolate and sodium methanolate [23], respectively. Subsequent couplings of the iodoazines **4a–4e** to the ethyne core existing in the target molecules **1a–1e** were performed, applying the metal-assisted Sonogashira–Hagihara cross-coupling procedure [24]. These couplings involve two individual steps and have been carried out using *trans*-dichlorobis(triphenylphosphine)palladium(II), copper(II) iodide, and triphenylphosphine in diisopropylamine as the catalytic system. To begin with, the respective iodoazines **4a–4e** were coupled with TMS-mono-protected ethyne to give the intermediate compounds **3a–3e**, which, after splitting off the TMS group, yielded the terminal acetylene derivatives **2a–2e**. These were subjected to an analogous cross-coupling reaction with the corresponding iodoazines **4a–4e** leading to **1a–1e**, which are new compounds, except **1b** that is known but has been synthesized on a different way [18]. On the whole, this methodic pathway for the preparation of symmetric ethynylene-bridged azines leads to considerable yields in view of the multi-step synthesis (Table 1).

Regarding the IR spectra of the compounds, the fourfold chlorinated bispyridine **1a** features a broad signal at 1103 cm^{-1} for the C–Cl stretching vibration, while the corresponding signals for **1b** (1017 cm^{-1}) and **1d** (1036 cm^{-1})

Table 1
Overall yields and melting points for the ethynyl-bridged bisazines **1a–1e**.

Compound	Synthetic steps	Overall yield (%)	Melting point (°C)
1a	4	15.7	140
1b	5	16.7	230
1c	5	42.4	57
1d	4	32.6	205
1e	5	32.9	182

sharpen and show decreasing intensity, respectively. The ^{1}H and ^{13}C NMR spectra of **1a–1e** largely correspond to the expected data. A more remarkable result, however, refers to the melting points determined for the bisazines **1a–1e** (Table 1). They differ broadly ranging between 57°C and 230°C. The highest melting points were found for **1b** (230°C) and **1d** (205°C), both being bisazines having the chloro substituents in linear fashion with reference to the ethynylene bond, while **1a** featuring the chlorine atoms in angular attachment to the molecular backbone shows a distinctly lower melting temperature of 140°C. This points to specific chlorine-involved interactions for **1a**, on the one side, or **1b** and **1d**, on the other side, in the crystalline state. Moreover, from spatial view, the nitrogen atoms in **1b** and **1d** should be more easily accessible to potential supramolecular interactions than in **1a**, pointing to the same fact. In the case of **1e** with polar methoxy groups linearly linked to the backbone structure, the melting point is moderately high (182°C). The lowest melting point applies to **1c** (57°C) being a reasonable implication of the bulky *tert*-butyl groups at the molecular periphery. In order to understand the solid state structures of the compounds **1a–1e** including argumentation of the supposed relations raised earlier, single-crystal X-ray structures have been performed.

X-ray crystallography. It is a well-known fact that supramolecular interactions such as hydrogen bonding [25], halogen bonding [26], and π···π contacts [27] are driving forces for the packing motif generated in a crystal. This is of relevance because the physical and physicochemical properties of a solid material are a direct consequence having both scientifically and economically great bearing, for example, in the preparation of pharmaceutical products and pigments, in many cases containing *N*-heterocycles and chlorine atoms in the molecular structure. Previous studies have shown that allowing a certain degree of predictability as far as the solid state structure is concerned, both knowledge of the supramolecular bonding capacity of the component building blocks and a controlled overall structure of the test molecule are promising. This is behind the concept of what is called "crystal engineering" [28]. However, many facts in particular connected with the competition problem between different modes of interaction that can potentially be formed are still not fundamentally understood, asking for further investigation. Following this idea, to study crystal structures of the present series of compounds may open valuable information considering that a variety of weak interactions involving X···X, C–H···X, X···π, C–H···π, and π···π contacts are likely competing for control of the crystal packing. Yet, compounds under discussion show rather defined molecular structures, making comparison reasonable. Aside from other relations, this may also suggest a potential background regarding the question raised with reference to the remarkably differing melting temperatures of the compounds under discussion. Hence, X-ray crystal structures of **1a–1e** have been studied.

Relevant crystallographic data and information concerning possible intermolecular interactions in the crystal structures are summarized in Tables 2 and 3. Molecular structures and packing diagrams are presented in Figures 1–8.

Crystal structures of the chloro-substituted dipyridinoethynes 1a and 1b. The tetrachloro-substituted dipyridylethyne **1a** crystallizes as colorless blocks of the tetragonal space group $I4_1/acd$ with one fourth of the molecule in the asymmetric part of the unit cell. The molecule adopts a distorted conformation with a twist angle of 19.5° between the aromatic rings (Fig. 1a). The bond distances within the molecular framework resemble those of 4,4′-dipyridylethyne being described in the literature as a component of some co-crystals [29,30].

Because of the irregular molecular conformation, undulated layers of molecules represent the basic supramolecular aggregates of the crystal structure (Fig. 2). Because of the steric demand of the two neighboring chlorine substituents, the nitrogen atoms are excluded from hydrogen bonding. Instead, ring motifs formed by four chlorine atoms [C(1)–Cl(1)···Cl(1) 3.560(1) Å, 151.6(1)°] represent the basic supramolecular contact mode within the molecular layer. In order to give a more detailed impression of this remarkable chlorine interaction, the electron density based on density functional theory was calculated using *quantum espresso* [31]. Figure 3 shows the respective cutout of the electron density map for the crystal structure of **1a**. Nevertheless, this particular type of cyclic Cl···Cl interaction is not an unknown phenomenon but has previously been observed also in a few aromatic structures [32,33] including a chlorine-containing bisazine [34]. Moreover, the chlorine atoms of the present structure take part in weak C–H···Cl contacts [35] [C(2)–H(2)···Cl(1) 2.99 Å, 140°]. In addition, offset face-to-face arene interactions [36] with a distance of approx. 3.4 Å between the interacting aromatic rings stabilize the crystal structure along the stacking axis of molecular layers.

The dichloro analogous derivative **1b** crystallizes as colorless plates of the triclinic space group *P*-1 with $Z = 1$. A perspective view of the molecular structure is depicted in Figure 1b. The molecule adopts a slightly

Table 2

Crystallographic and structure refinement data of the compounds studied.

Compound	1a	1b	1c	1d	1e
Empirical formula	$C_{12}H_4Cl_4N_2$	$C_{12}H_6Cl_2N_2$	$C_{18}H_{22}N_4S_2$	$C_{10}H_4Cl_2N_4$	$C_{12}H_{10}N_4O_2$
Formula weight (g mol^{-1})	317.97	249.09	358.52	251.07	242.24
Crystal system	Tetragonal	Triclinic	Monoclinic	Monoclinic	Monoclinic
Space group	*I*4(1)/*acd*	*P*-1	$P2_1/n$	$P2_1/n$	$P2_1/c$
a (Å)	14.0256(2)	3.8412(2)	5.9441(2)	4.65630(10)	3.9098(3)
b (Å)	14.0256(2)	5.7910(2)	15.7221(4)	10.2482(3)	14.3917(8)
c (Å)	12.5945(2)	12.5619(5)	20.4018(5)	10.9571(3)	10.0630(6)
α (°)	90.00	83.430(3)	90.00	90.00	90.00
β (°)	90.00	86.370(3)	94.2120(10)	98.106(1)	98.171(3)
γ (°)	90.00	76.128(3)	90.00	90.00	90.00
V (Å^3)	2477.56(6)	269.31(2)	1901.47(9)	517.63(2)	560.48(6)
Z	8	1	4	2	2
F(000)	1264	126	760	252	252
D_c (Mg m^{-3})	1.705	1.536	1.252	1.611	1.435
μ (mm^{-1})	0.934	0.571	0.287	0.600	0.103
Data collection					
Temperature (K)	100(2)	296(2)	100(2)	296(2)	296(2)
No. of collected reflections	12804	4139	50679	12407	4726
Within the θ-limit (°)	3.6–37.6	3.3–28.4	2.4–34.1	2.7–30.6	2.5–26.6
Index ranges $\pm h$, $\pm k$, $\pm l$	−24/23, −15/24, −17/21	−5/5, −7/7, −16/16	−9/5, −23/24, −31/32	−6/6, −14/14, −15/15	−4/4, −15/18, −11/12
No. of unique reflections	1645	1338	7820	1594	1169
R_{int}	0.0197	0.0210	0.0267	0.0192	0.0255
Weighting expression *w*[a]	$[\sigma^2(F_o^2)+(0.0361P)^2+0.8451P]$	$[\sigma^2(F_o^2)+(0.0287P)^2+0.1041P]$	$[\sigma^2(F_o^2)+(0.0366P)^2+0.6389P]$	$[\sigma^2(F_o^2)+(0.0811P)^2+0.1028P]$	$[\sigma^2(F_o^2)+(0.0523P)^2+0.0951P]$
No. of refined parameters	43	73	223	73	83
No. of *F* values used [$I > 2\sigma(I)$]	1492	1020	6816	1376	823
Final *R*-indices					
$R(=\sum\|\Delta F\|/\sum\|F_o\|)$	0.0223	0.0343	0.0283	0.0386	0.0394
wR on F^2	0.0683	0.0865	0.0771	0.1352	0.1125
S (=goodness of fit on F^2)	1.123	1.053	0.950	1.055	1.054
Final $\Delta\rho_{max}/\Delta\rho_{min}$ (e Å^{-3})	0.579/−0.326	0.219/−0.202	0.461/−0.236	0.313/−0.191	0.173/−0.148
KPI index [44] %	71.3	70.6	66.6	70.6	72.1

[a] $P = (F_o^2 + 2F_c^2)/3$.

Table 3

Geometric parameters for intermolecular contacts in compounds studied in this article.

Atoms involved	Symmetry	Distance (Å) D–H C–X	Distance (Å) D···A C···A	Distance (Å) H···A X···A	Angle (°) D–H···A C–X···A
1a					
C(2)–H(2)···Cl(1)	$-3/4+y$, $7/4-x$, $1/4-z$	0.95	3.649(1)	2.99	140
C(1)–Cl(1)···Cl(1)	$7/4-y$, $3/4+x$, $1/4-z$	1.731(1)		3.560(1)	151.6(1)
C(1)–Cl(1)···cg(A)[a]	x, $2-y$, $1/2-z$	1.731(1)	3.482(1)	3.789 (1)	66.50(2)
cg(A)···cg(A)[a]	x, $2-y$, $1/2-z$			3.823(1)	
1b					
C(1)–Cl(1)···Cl(1)	$-x$, $2-y$, $-z$	1.738(2)		3.349 (2)	160.6(1)
C(4)–H(4)···N(1)	$1+x$, $-1+y$, z	0.93	3.409(2)	2.51	161
cg(A)···cg(A)				3.841(2)	
1c					
C(13)–H(13A)···N(1)	x, y, z	0.98	3.159(1)	2.48	126
C(12)–H(12C)···N(1)	x, y, z	0.98	3.139(1)	2.45	127
C(16)–H(16C)···N(3)	x, y, z	0.98	3.186(1)	2.50	127
C(17)–H(17A)···N(3)	x, y, z	0.98	3.130(1)	2.44	127
C(8)–H(8)···N(4)	$-1+x$, y, z	0.95	3.302(1)	2.42	155
C(16)–H(16A)···cg(A)[a]	$1/2+x$, $3/2-y$, $1/2+z$	0.98	3.641(1)	2.69	163
cg(B)···cg(B)[a]	$1-x$, $2-y$, $2-z$			3.9384(5)	
1d					
C(4)–H(4)···Cl(1)	$1/2-x$, $-1/2+y$, $1/2-z$	0.93	3.462(2)	3.00	112
C(1)–Cl(1)···cg(A)[a]	x, y, z	1.729(1)		3.5366(7)	90.51(5)
C(2)–H(2)···N(2)	$-1/2+x$, $3/2-y$, $1/2+z$	0.93	3.645( )	2.80	152
cg(A)···cg(C≡C)	$2-x$, $2-y$, $-z$		3.593(2)		
1e					
C(6)–H(6C)···O(1)	$1+x$, y, z	0.96	3.255(2)	2.69	151
C(4)–H(4)···N(1)	$-1+x$, $3/2-y$, $-1/2+z$	0.93	3.444(2)	2.67	146
C(1)–O(1)···O(1)	$1-x$, $2-y$, $-z$	1.333(2)		2.864(2)	145
cg(A)···cg(A)				3.910(2)	

[a]cg means center of the aromatic rings. Ring A: N1–C1–C2–C3 (**1a**), C1–N1–C2–C3–C4–C5 (**1b**), N1–C1–C2–C3–C4–N2 (**1c–1e**). Ring B: C7–C8–N3–C9–N4–C10 (**1c**).

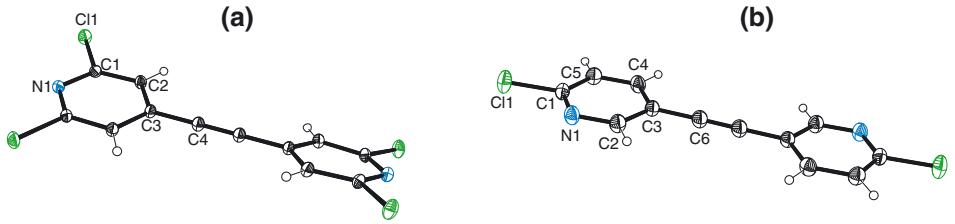

Figure 1. Perspective views of **1a** (a) and **1b** (b), including the numbering scheme of atoms. Thermal ellipsoids are drawn at 50% (**1a**) and 30% (**1b**) probability level.

distorted conformation along its main axis, which is obvious from the bond angles around the substituted ring carbon atoms C(1) and C(3) [N(1)–C(1)–Cl(1) 115.7 (2) Å, C(4)–C(3)–C(6) 122.1(2)°]. The bond lengths agree with those of the unsubstituted parent molecule [37]. The crystal structure (Fig. 4) is composed of infinite C–H···N bonded [38] strands [C(4)–H(4)···N(1) 2.51 Å, 161°], which are further associated *via* Cl···Cl interactions [39] [C(1)–Cl(1)···Cl(1) 3.349(2) Å, 160.1(1)°] to form two-dimensional molecular networks extending parallel to the crystallographic 112 plane. According to their geometry, the Cl···Cl interactions meet the conditions of a type I (head-on) contact very well [39].

Crystal structures of the substituted dipyrimidinoethynes 1c–1e. Perspective views of the molecular structures of **1c–1e** are displayed in Figure 5. The bond lengths within the diarylethynylene framework of the molecules are in the range of those found for the unsubstituted parent compound 1,2-bis(pyrimid-5-yl)ethyne [17]. This means that substituents of different electronic nature hardly affect bond distances. The *t*-butylthio-substituted compound **1c** exists in the monoclinic space group $P2_1/n$ ($Z=4$) with the

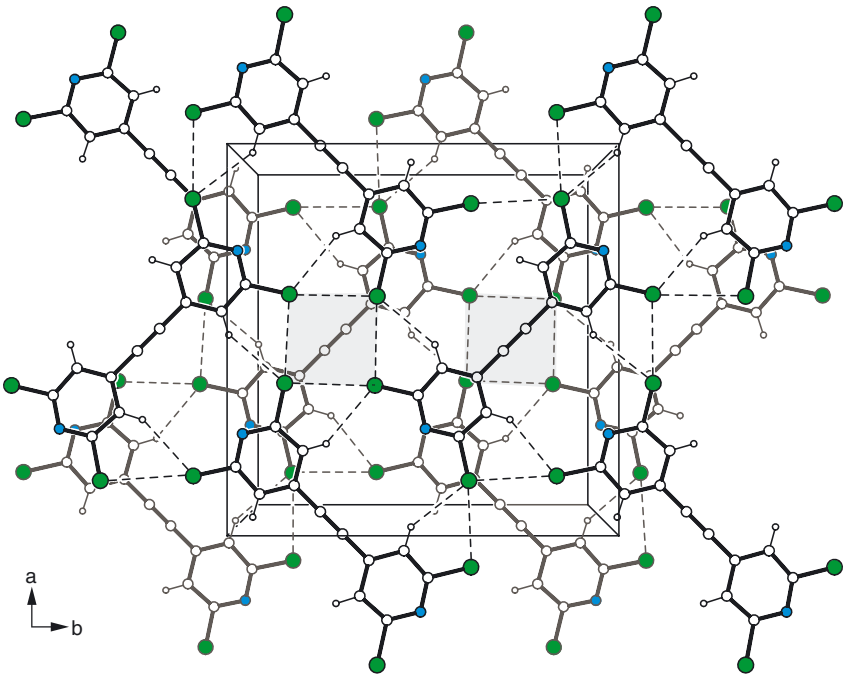

Figure 2. Packing structure of **1a** viewed down the crystallographic *c*-axis. Broken lines represent C–H···Cl and Cl···Cl contacts. The tetra-chlorine-containing ring motif is indicated by shading.

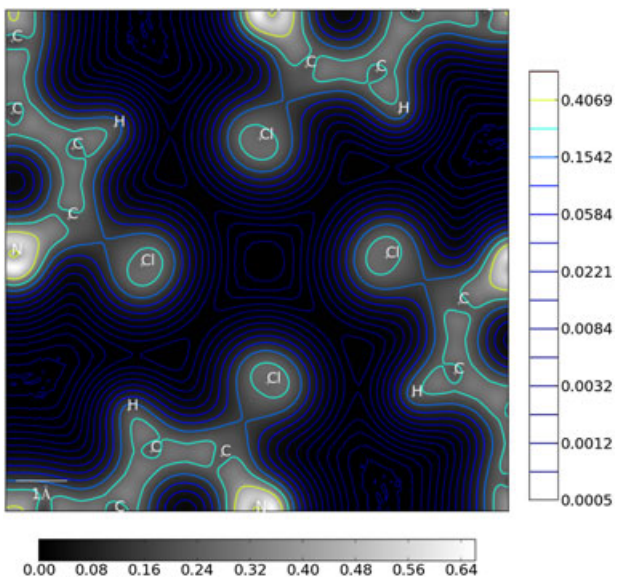

Figure 3. Cutout of the electron density map for the crystal structure of **1a**. The electron density was calculated using a GGA exchange-correlation functional after Perdew–Burke–Ernzerhof [49]. Electron density values are given in $e \cdot a_0^{-3}$.

molecule located in a general position. The twist angle between the aromatic rings is 12.0(1)°. The molecular conformation is determined by four intramolecular C–H···N hydrogen bond type contacts involving *tert*-butyl hydrogens as donors and the nitrogens N(1) and N(3) as acceptor sites [*d*(C···N) 3.130(1), 3.186(1) Å]. Crystals of the methoxy- and chlorine-substituted derivatives **1e** and **1d** have the monoclinic space groups $P2_1/c$ and $P2_1/n$, respectively, with $Z = 2$; that is, the molecules are located on symmetry centers. Hence, the molecular backbone is of approximate planarity.

In the crystal structure of **1c**, the molecule adopts a distorted conformation that may be ascribed to packing effects caused by the bulky *tert*-butyl terminal groups. As shown in Figure 6, the crystal structure is composed of C–H···N bonded molecular tapes [C(8)–H(8)···N(4) 2.42 Å, 155°] running along the crystallographic *a*-axis. Within these aggregates, molecules are linked in an asymmetric fashion because only one nitrogen of each molecule is involved in intermolecular hydrogen bonding. Also, the aromatic rings are involved in a different way in intermolecular interactions. The mean distance of approx. 3.30 Å between the aromatic units of adjacent molecular tapes suggests the presence of offset face-to-face π···π arene interactions. In addition, the crystal structure is stabilized by multiple C–$H_{t\text{-butyl}}$···π_{arene} contacts [25].

The crystal structure of **1d** is constructed of molecular stacks extending along the *a*-axis (Fig. 7). Within a given stack, consecutive molecules are displaced in the direction of their longitudinal axes. In this arrangement, the ethynylene unit of each molecule is located between the aromatic rings of neighboring molecules indicating the presence of π_{arene}···π_{ethyne} interactions [cg(A)···cg(C≡C) 3.593(2) Å]. Molecules of neighboring stacks are inclined at approximately 75° to one another, possibly to realize a close packing

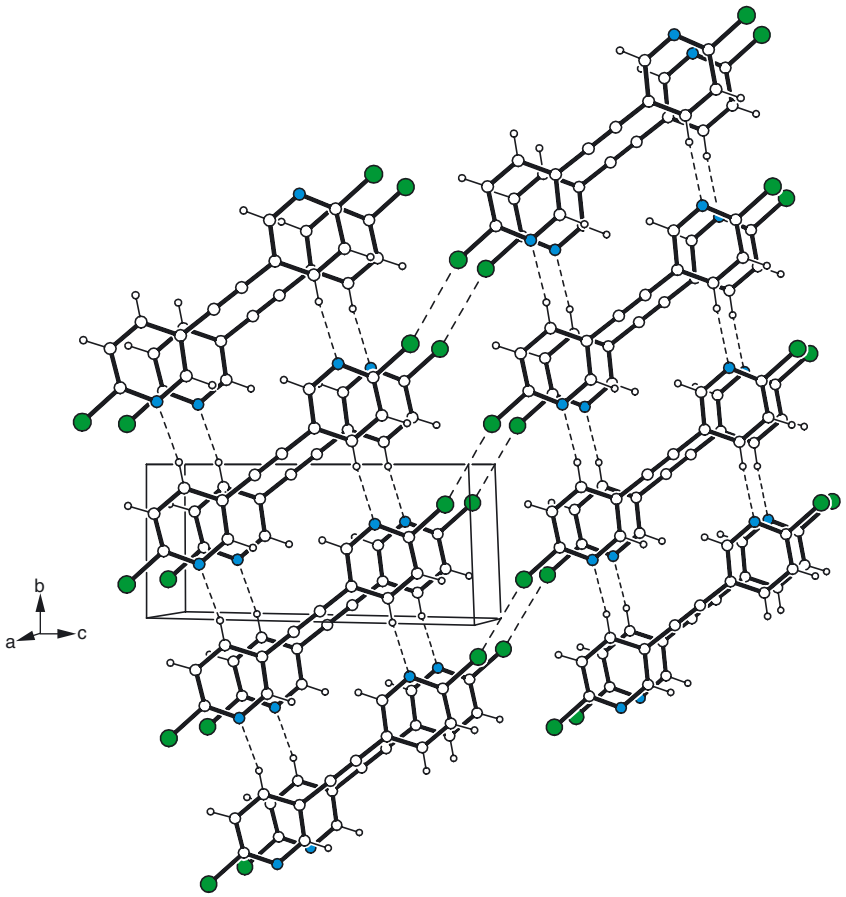

Figure 4. Packing structure of **1b**. C–H···N and halogen interactions are marked by broken lines.

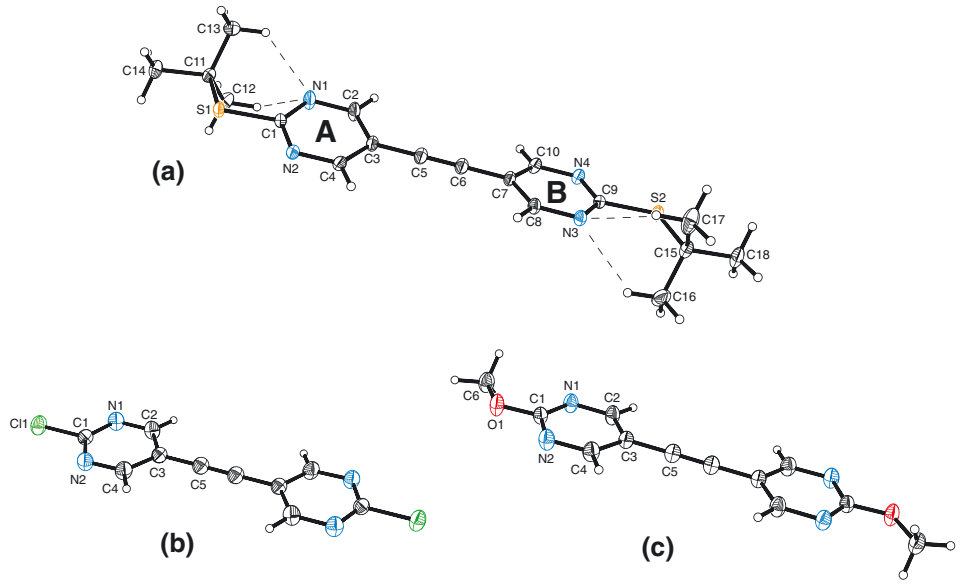

Figure 5. Perspective views of **1c** (a), **1d** (b), and **1e** (c), including the numbering scheme of atoms. Thermal ellipsoids are drawn at 50% (**1c**) and 30% (**1d/e**) probability level.

structure. In a similar fashion as in the aforementioned case, one of the pyrimidine nitrogens is involved in intermolecular association giving rise to weak C–H···N hydrogen bond [C(2)–H(2)···N(2) 2.80 Å, 152°] that interlinks the molecular

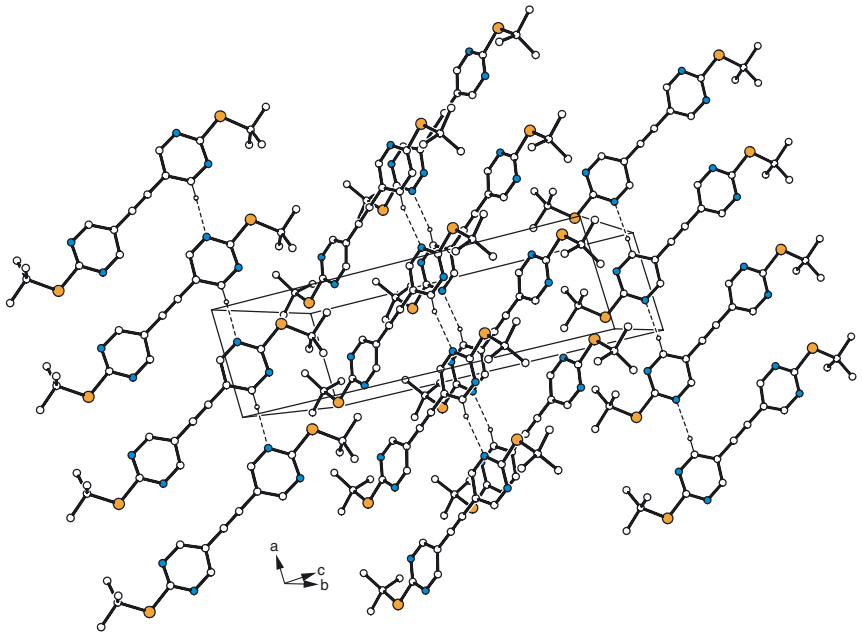

Figure 6. Packing structure of **1c**. All hydrogen atoms except those involved in C–H···N interaction (broken lines) are omitted for clarity.

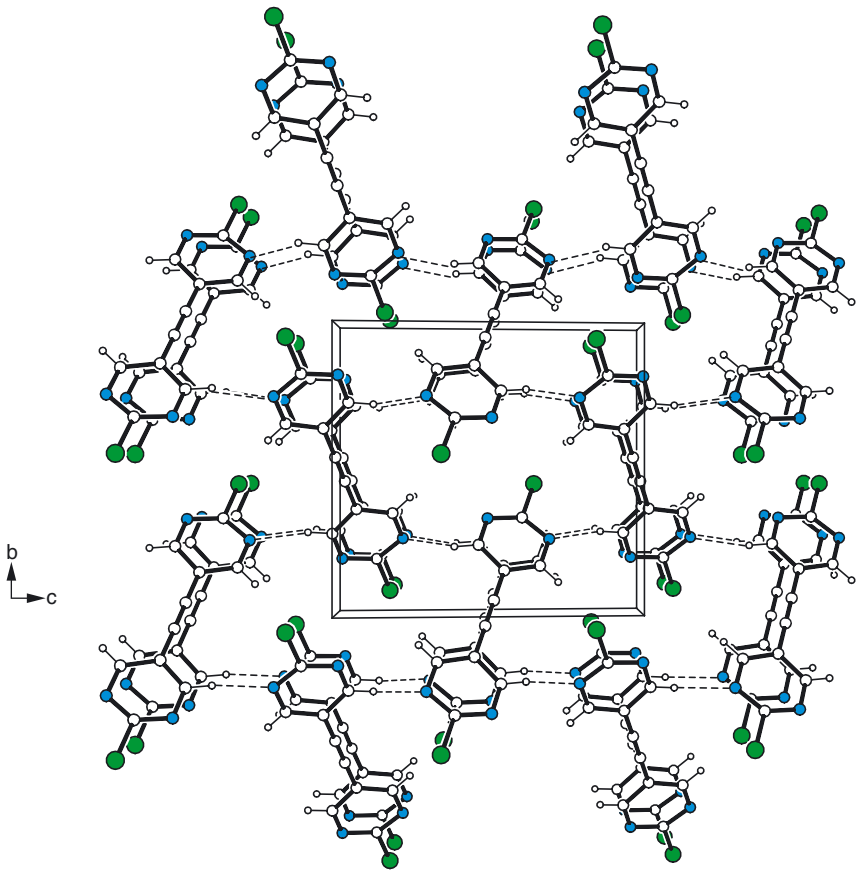

Figure 7. Packing structure of **1d** viewed down the crystallographic *a*-axis. Broken lines represent hydrogen bond type interactions.

stacks. Noteworthy enough, there is no short contact in the structure to be assigned a Cl···Cl interaction.

A view of the crystal structure of **1e** along the crystallographic *b*-axis reveals a layered packing of molecules

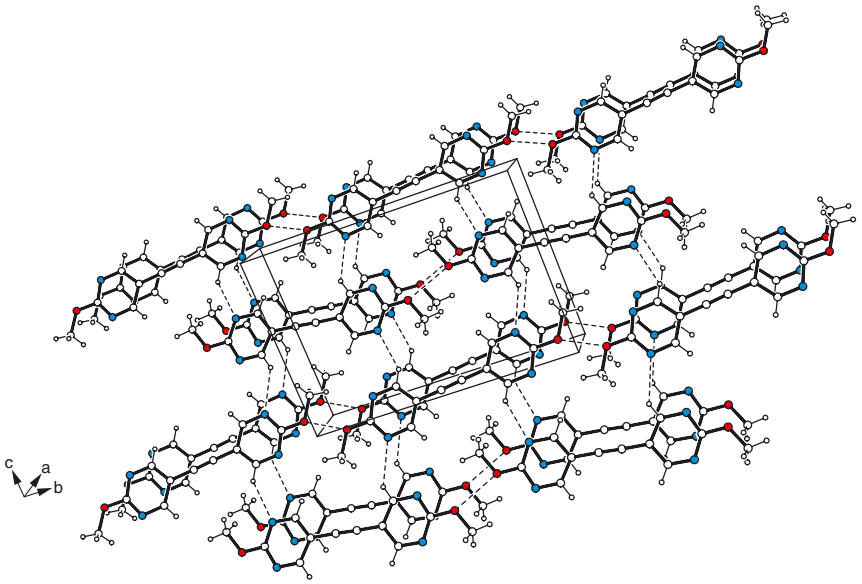

Figure 8. Packing structure of **1e**. Broken lines represent hydrogen bond type and O···O contacts.

(Fig. 8). Each layer is composed of parallel C–H···N bonded molecular strands in which only one of the pyrimidine nitrogens participates in this contact [C(4)–H(4)···N(1) 2.67 Å, 146°]. A remarkable O···O distance of 2.864(2) Å between molecules of adjacent strands falling short of twice the van der Waals radius of oxygen (1.52 Å) suggests the presence of weak intermolecular O···O contacts. However, a couple of structures showing this particular type of interaction mainly supported by phenolic oxygen atoms located in the β-position of one or more nitrogen atoms can already be found in the literature [40–42]. Offset face-to-face arene interactions with a distance of approx. 3.5 Å between the planes of adjacent molecules stabilize the packing structure along the stacking axis of the supramolecular layers.

COMPARATIVE REFLECTION AND CONCLUSIONS

Using a Pd-catalyzed coupling procedure as key step of the synthesis, a series of five bispyridine and bispyrimidine derivatives featuring the heterocycles attached to a central acetylene unit and having chlorine, *tert*-butylthio, or methoxy groups as additional substituents were successfully prepared. These compounds not only show promising structural property for the potential use as linker-type molecules in the construction of coordination polymers or related supramolecular architectures but offer also an interesting cooperative study of their solid state structures, giving rise to conclusions that should be of use in this field of heterocyclic chemistry.

Considering the molecular conformations of the compounds, the heterocyclic rings are largely coplanar and show only in the cases of the tetrachloro derivative **1a** and the bulkily *tert*-butylthio-substituted molecule **1c** a moderate deviation from coplanarity that might be a result of packing effects caused by the specific substitutions. Another active part in the conformational behavior of **1c** may be ascribed to the intramolecular H-bonds of inverse bifurcated nature being formed between methyl groups and one of the pyrimidine nitrogens of both terminals of the molecule, thus preventing the *tert*-butyl groups from rotation. Although C–H···N hydrogen bonding of ring type $R_2^1(6)$ is known on principle, a similar situation involving a *tert*-butyl group has not been described before.

Regarding the supramolecular interactions, C–H···N contacts play a dominating role in all structures excepting **1a** where the nitrogens seem to be shielded from interaction by the neighboring chlorines. In the crystal structures of **1b–1e**, these C–H···N contacts give rise to different modes of supramolecular netting. That is, in the cases of **1b** and **1c**, tapes of parallel aligned molecules are formed with each molecule interacting in both directions only with one neighboring molecule, while in the crystals of **1d** and **1e**, the structures are more complex because the interacting molecules are displaced against each other, creating hydrogen bonds to four different neighbors. The tapes of **1b** are linked *via* head-on Cl···Cl contacts to yield planes that stack in aromatic π···π interaction mode. Also, in **1c** aromatic π···π stacking, interactions and weak C–H···π contacts participate in the stabilization of the tapes. In **1d**, the structure is stabilized by additional Cl···π, C–H···Cl, and π(arene)···π(ethynyl) contacts, and **1e** shows plane formation created by a combination of the C–H···N interaction with linear O···O contacts giving rise to stacking of the planes. Hence, all the structures of **1b–1e** are dominated by C–H···N and π···π stacking contacts including supportive

interactions such as Cl···Cl (**1b**), weak C–H···π (**1c**), Cl···π and C–H···Cl (**1d**), or O···O type (**1e**) according to the compound species.

Another result follows from comparison of the crystal structures of chloro-substituted compounds **1a**, **1b**, and **1d**. Although in all their structures the chlorine atoms are involved in intermolecular interactions, modes of contact are different; that is, weak C–H···Cl and Cl···π contacts in the case of **1d** while both in **1a** and **1b** the Cl atoms give rise to Cl···Cl interactions. Nevertheless, in **1b**, these Cl···Cl contacts are type I (head-on) mode but in **1a** type II (side-on) mode, suggesting specific exerting of influence of the chlorine's disposition and vicinity in the molecule on the halogen interaction. In the case of **1a**, this leads to the remarkable formation of a square of four contacting halogen atoms nevertheless, which is typical enough recently being suggested as a potential supramolecular synthon of halogen interaction in crystals [43].

Correlations between the marked differences in melting points among the compounds mentioned earlier and their crystal structures are not readily obvious but might be reflected as follows. In the structures of compounds **1b**, **1d** and **1e**, showing the highest temperature of melting, three-dimensional networks involving distinct C–H···N and π···π interactions supported by additional heteroatom contacts are observed. However, **1c**, having the lowest melting point, yields only half as much of C–H···N contacts per molecule because only one of the heteroaromatic rings is included and only weak C–H···π contacts are present for additional support of the structure. The structure of the bisazine **1a** with moderate temperature of melting between that of **1c** and the other compounds does not show the prior C–H···N contacts. In this connection, it is also interesting to note that just the compounds **1a** and **1c**, having the lowest melting points, are those featuring an interplanar angle of the azine rings considerably different from coplanarity, which suggests some strain in the packing possibly becoming apparent in lower temperature of melting because of destabilization of the crystal lattice. The packing densities (KPI index [44] %) for all crystals were calculated as 71.3 (**1a**), 70.6 (**1b**), 66.6 (**1c**), 70.6 (**1d**), and 72.1 (**1e**). Used as a further potential way of argumentation, they indicate a distinctly lower value for **1c** compared with the other compounds, which is in agreement with the particularly low melting temperature of **1c**, but more clearly perceptible correlation seems hardly readable from the data.

EXPERIMENTAL

General. Melting points: Kofler melting point microscope (uncorrected). IR: Nicolet FT-IR 510. ^{1}H and ^{13}C NMR (internal standard TMS, δ in ppm): Bruker AVANCE DPX 500. MS (ESI): Varian 320 MS [CID 100 V, solvent: methanol/water (9 : 1)]. Elemental analysis: Hanau vario MICRO cube. Column chromatography: silica gel 60 (0.040–0.063 mm, Merck). TLC analysis: aluminum sheets precoated with silica gel 60 F254 (Merck).

Reagents and materials were obtained from commercial suppliers (Fisher Scientific, ABCR, Aldrich) and were used without further purification. The solvents were purified using standard procedures. Solvents for the Sonogashira–Hagihara coupling reactions were deoxygenated prior to use by ultrasound (20 min) while bubbling argon through the solution.

2-Hydroxy-5-iodopyridine (5). To 34.9 g (0.4 mol) 2-hydroxypyridine dissolved in 650 mL methanol, 56.0 g (0.4 mol) sodium iodide and 14.7 g (0.4 mol) sodium hydroxide were added at 0°C. Following, 677.7 g (0.4 mol) of an aqueous sodium hypochlorite solution (4% active chlorine) was added dropwise over 2 h at 40°C, and the mixture was stirred for another 2 h at room temperature. After that, 350 mL of a 0.6 *M* aqueous sodium thiosulfate solution was added, and the mixture was neutralized with 300 mL of aqueous 1.4 *M* hydrochloric acid. Evaporation of the methanol *in vacuo* yielded a white precipitate. This was separated from the liquid phase and washed with water to give 48.6 g (60%) of the pure product, mp 190°C (Lit.: 190–191°C [20]), ^{1}H NMR (DMSO-d_6): δ 8.60 (d, ^4J = 2.2 Hz, 1 H, phenyl), 7.92 (dd, ^3J = 8.3 Hz, ^4J = 2.2 Hz, 1 H, phenyl), 7.14 (d, ^3J = 8.3 Hz, 1 H, phenyl); ^{13}C NMR (DMSO-d_6): δ 161.9, 147.6, 140.0, 121.6, 64.4.

2,6-Dichloro-4-iodopyridine (4a). 7.5 g (0.05 mol) 2,6-dichloropyridine was dissolved in 85 mL tetrahydrofuran and cooled down to −75°C. To this solution, 32 mL of a 1.6 *M* *n*-BuLi solution in *n*-hexane was added, and the resulting mixture was stirred for 45 min at −75°C. Following, a solution of 13.0 g (0.1 mol) iodine in 24 mL tetrahydrofuran was added dropwise, and stirring was continued for another 15 min at −75°C. The solution was allowed to warm to room temperature and treated with 43 mL of aqueous 0.6 *M* sodium thiosulfate and water. After removal of the solvent, a mixture consisting of 2,6-dichloro-4-iodopyridine and 2,6-dichloro-3-iodopyridine as by-product was obtained. Fractional crystallization from dry ethanol yielded 4.1 g of the title compound as white, crystalline solid (30%), mp 162°C (Lit.: 162–164°C [19]), ^{1}H NMR ($CDCl_3$): δ 7.66 (s, 1 H phenyl); ^{13}C NMR ($CDCl_3$): δ 150.7, 131.5, 107.6.

General procedure for preparation of 4b and 4d. The respective 2-hydroxyazine was suspended in dry acetonitrile, and a 1.3 times excess of phosphorous oxychloride was added in one bulk. Subsequently, the equimolar amount of *N*,*N*-diisopropylethylamine was added dropwise, and the reaction mixture was stirred under reflux (time of stirring as specified for each compound). After cooling to approx. 40°C, an equal volume of water was added dropwise over 20 min. Both the resulting residue and the filtrate were extracted with ethyl acetate. To the combined organic layers, water (10% by volume of the organic phase) was added, and the resulting inhomogenous mixture was evaporated until the inner temperature reached 85°C. Cooling to room temperature yielded the crude product as a white precipitate, which was purified by crystallization from *n*-hexane. Specific details for each compound are specified in the following sections.

2-Chloro-5-iodopyridine (4b). 10.0 g (45.5 mmol) 5-iodo-2-hydroxypyridine (**5**) was reacted in 80 mL acetonitrile for 4 h yielding 8.0 g (74%), mp 98°C (Lit.: 98°C [45]), ^{1}H NMR ($CDCl_3$): δ 8.60 (d, 1 H, ^4J = 2.2 Hz, phenyl), 7.92 (dd, 1 H,

$^3J = 8.3$ Hz, $^4J = 2.2$ Hz, phenyl), 7.14 (d, 1 H, $^3J = 8.3$ Hz, phenyl); ^{13}C NMR ($CDCl_3$): δ 155.6, 150.9, 146.7, 126.1, 90.7.

2-Chloro-5-iodopyrimidine (4d). 50.0 g (0.2 mol) 5-iodo-2-hydroxypyrimidine were reacted in 270 mL acetonitrile for 20 h using the chlorination procedure yielding 48.5 g (90%, Lit.: 72% [22]), mp 133°C (Lit.: 129–130°C [46]), ^{1}H NMR (DMSO-d_6): δ 9.04 (s, 2 H, phenyl); ^{13}C NMR (DMSO-d_6): δ 165.5, 159.0, 93.0.

2-(t-Butylthio)-5-iodopyrimidine (4c). To 0.8 g (21.0 mmol) of a 60% dispersion of sodium hydride in mineral oil dissolved in 50 mL of dry dimethyl formamide, 1.9 g (21.0 mmol) 2-methylpropane-2-thiol was added dropwise. The mixture was stirred for 30 min at room temperature. Then, 5.0 g (21.0 mmol) 2-chloro-5-iodopyrimidine (**4d**) was added, and the resulting suspension was stirred for 2 h at room temperature. The solvent was removed *in vacuo*, and the residue treated with 100 mL of water and extracted with diethyl ether. Purification by column chromatography (SiO_2; *n*-hexane/ethyl acetate; 50 : 1) yielded 5.3 g (85%) of a white solid, mp 38°C, IR: CH 3229, ArCH 3079, CN 1698, CH 1394, CI 1071 cm^{-1}; ^{1}H NMR ($CDCl_3$): δ 8.66 (s, 2 H, phenyl), 1.59 (s, 9 H, CH_3). ^{13}C NMR ($CDCl_3$): δ 171.4, 161.5, 86.1, 47.2, 29.5; MS: *m*/*z* 295 (M^+).

5-Iodo-2-methoxypyrimidine (4e). To a suspension of 8.8 g (36.8 mmol) 2-chloro-5-iodopyrimidine (**4d**) in 40 mL of dry methanol, a methanolic sodium methanolate solution [obtained from 1.0 g (43.5 mmol) sodium in 50 mL dry methanol] was added dropwise. After having stirred for 2 h at room temperature, the mixture was evaporated *in vacuo*. The residue was treated with 60 mL of water and extracted with methylene chloride. The combined organic layers were dried over sodium sulfate and evaporated to dryness to give 8.2 g (94%, Lit.: 80% [23]) of a white solid, mp 125°C, ^{1}H NMR ($CDCl_3$): δ 8.65 (s, 2 H, phenyl), 3.99 (s, 3H, CH_3); ^{13}C NMR ($CDCl_3$): δ 165.5, 159.0, 93.0.

Sonogashira–Hagihara coupling procedure. The respective aryl iodide and the corresponding terminal alkynyl component were dissolved in a degassed mixture of diisopropylamine and tetrahydrofuran. To this solution, the catalyst, being composed of triphenylphosphine (2 mol-%), copper(I) iodide (3 mol-%), and *trans*-dichlorobis-(triphenylphosphine)palladium(II) (2 mol-%), was added and the mixture stirred until completion of the reaction (TLC analysis). Evaporation of the solvent followed by column chromatography and/or crystallization yielded the pure compounds. Specific details for each compound are given in the following sections.

2,6-Dichloro-4-(trimethylsilylethynyl)pyridine (3a). 5.0 g (18.3 mmol) 2,6-dichloro-4-iodopyridine (**4a**), 1.9 g (19.0 mmol) trimethylsilyl acetylene, and the catalyst in a mixture of 120 mL diisopropylamine and 120 mL tetrahydrofuran were used. After stirring for 3 h at room temperature, the reaction was complete. Purification by column chromatography (SiO_2; *n*-hexane/ethyl acetate; 50 : 1) yielded 2.4 g (54%) of a colorless oil, ^{1}H NMR ($CDCl_3$): δ 7.28 (s, 2 H, phenyl), 0.26 (s, 9 H, CH_3); ^{13}C NMR ($CDCl_3$): δ 151.3, 136.7, 125.7, 104.2, 99.8, 0.0.

2-Chloro-5-(trimethylsilylethynyl)pyridine (3b). 9.0 g (37.7 mmol) 2-chloro-5-iodopyridine (**4b**), 3.9 g (40.0 mmol) trimethylsilyl acetylene, and the catalyst in a mixture of 250 mL diisopropylamine and 250 mL tetrahydrofuran were used. After reflux for 4 h, the reaction was complete. Purification by column chromatography (SiO_2; *n*-hexane/ethyl acetate; 20 : 1) yielded 5.9 g (75%) of a white solid, mp 59°C, ^{1}H NMR ($CDCl_3$): δ 8.46 (d, 1 H, $^4J = 2.1$ Hz, phenyl), 7.68 (dd, 1 H, $^3J = 8.3$ Hz, $^4J = 2.1$, phenyl), 7.27 (d, 1 H, $^3J = 8.3$ Hz, phenyl), 0.26 (s, 9 H, CH_3); ^{13}C NMR ($CDCl_3$): δ 152.4, 150.5, 141.2, 123.7, 119.1, 100.0, 99.6, −0.3.

2-(t-Butylthio)-5-(trimethylsilylethynyl)pyrimidine (3c). 10.0 g (34.0 mmol) 2-(*t*-butylthio)-5-iodopyrimidine (**4c**), 3.5 g (35.5 mmol) trimethylsilyl acetylene, and the catalyst in a mixture of 240 mL diisopropylamine and 240 mL of tetrahydrofuran were used. After stirring at room temperature for 6 h, the reaction was complete. Purification by column chromatography (SiO_2; *n*-hexane/ethyl acetate; 20 : 1) yielded 6.7 g (75%) of a white solid, mp 28°C; IR: ArCH 2957, CC 2161, CN 1572, CH 1396 cm^{-1}; ^{1}H NMR ($CDCl_3$): δ 8.53 (s, 2 H, phenyl), 1.61 (s, 9 H, CH_3), 0.26 (s, 9 H, CH_3); ^{13}C NMR ($CDCl_3$): δ 171.9, 158.8, 113.9, 101.0, 98.3, 47.7, 29.8, 29.8; MS: *m*/*z* 265 (M^+).

2-Chloro-5-(trimethylsilylethynyl)pyrimidine (3d). 2.0 g (8.4 mmol) 2-chloro-5-iodopyrimidine (**4d**), 0.9 g (9.0 mmol) trimethylsilyl acetylene, and the catalyst in 60 mL diisopropylamine were used. After stirring at room temperature for 12 h, the reaction was complete. Purification by recrystallization from *n*-hexane yielded 1.8 g (99%) of a white solid, mp 48°C, ^{1}H NMR ($CDCl_3$): δ 8.70 (s, 2 H, phenyl), 3.47 (s, 1 H, CH); ^{13}C NMR ($CDCl_3$): δ 161.7, 160.1, 117.2, 85.6, 75.7.

2-Methoxy-5-(trimethylsilylethynyl)pyrimidine (3e). 4.0 g (17.0 mmol) 5-iodo-2-methoxypyrimidine (**4e**), 1.7 g (17.0 mmol) trimethylsilyl acetylene, and the catalyst in 120 mL diisopropylamine were used. After stirring at room temperature for 3 h, the reaction was complete. Purification by column chromatography (SiO_2; *n*-hexane/ethyl acetate; 9 : 1) yielded 3.0 g (87%) of a white solid, mp 42°C, ^{1}H NMR ($CDCl_3$): δ 8.58 (s, 2 H, phenyl), 4.03 (s, 3 H, CH_3), 0.26 (s, 9 H, CH_3); ^{13}C NMR ($CDCl_3$): δ 164.2, 163.9, 161.7, 112.8, 99.9, 97.9, 55.2, 0.3.

General procedure for cleavage of the trimethylsilyl group. To the TMS-protected acetylene dissolved in acetonitrile, potassium hydroxide at 5 *M* aqueous solution was added at 0°C. The solution was stirred for 15 min at this temperature and poured into water. In the case of precipitation, the solid was separated, washed with water, and dried on air. Otherwise, the resulting solution was extracted with diethyl ether, dried (Na_2SO_4), and evaporated. Purification was accomplished by further extraction or sublimation. Specifications for each compound are given in the following sections.

2,6-Dichloro-4-ethynylpyridine (2a). 2.1 g (8.5 mmol) 2,6-dichloro-4-(trimethylsilylethynyl)pyridine (**3a**) in 50 mL acetonitrile and 17 mL of the KOH solution was used. Purification by sublimation at 80°C (15 Torr) yielded 1.4 g (93%) of a white solid, mp 86°C, ^{1}H NMR ($CDCl_3$): δ 7.32 (s, 2 H, phenyl), 3.42 (s, 1 H, CH); ^{13}C NMR ($CDCl_3$): δ 150.8, 135.2, 125.1, 84.6, 78.6.

2-Chloro-5-ethynylpyridine (2b). 4.2 g (20.0 mmol) 2-chloro-5-(trimethylsilylethynyl)pyridine (**3b**) in 40 mL acetonitrile and 40 mL of the KOH solution was used. Purification by extraction with diethyl ether yielded 2.1 g (75%) of a white solid, mp 82°C, ^{1}H NMR ($CDCl_3$): δ 8.49 (d, 1 H, $^4J = 2.3$ Hz, phenyl), 7.72 (dd, 1 H, $^3J = 8.2$ Hz, $^4J = 2.3$ Hz, phenyl), 7.30 (d, 1 H, $^3J = 8.2$ Hz, phenyl), 3.28 (s, 1 H, CH); ^{13}C NMR ($CDCl_3$): δ 152.4, 150.5, 141.2, 123.7, 119.1, 100.0, 99.6, −0.3.

2-(t-Butylthio)-5-ethynylpyrimidine (2c). 6.0 g (22.7 mmol) 2-(*t*-butylthio)-5-(trimethylsilylethynyl)pyrimidine (**3c**) in 90 mL acetonitrile and 45 mL of the KOH solution was used. Purification by extraction with diethyl ether yielded 4.2 g (96%) of a white solid, mp 32°C, IR: CH 3229, ArCH 2961, CC 2112, CN 1571, CH 1398 cm^{-1}; ^{1}H NMR ($CDCl_3$): δ 8.57 (s, 2 H, phenyl), 3.33 (s, 1 H, CH), 1.62 (s, 9 H, CH_3); ^{13}C NMR ($CDCl_3$) δ 172.7,

159.0, 112.9, 83.1, 77.1, 47.8, 29.9; MS: *m/z* 193 (M^+); *Anal.* Calcd. for $C_{10}H_{12}N_2S$ (192.07): C, 62.46; H, 6.29; N, 14.57; S, 16.68; Found: C, 62.39; H, 6.45; N, 14.69; S, 16.74%.

2-Chloro-5-ethynylpyrimidine (2d). 4.0 g (4.8 mmol) 2-chloro-5-(trimethylsilylethynyl)pyrimidine (**3d**) in 15 mL acetonitrile and 10 mL of the KOH solution was used. Purification by extraction with diethyl ether yielded 2.3 g (60%) yellow needles, mp 140°C, IR: CH 3212, ArCH 3037, CC 2107, CN 1568, CCl 1036 cm^{-1}; ^1H NMR ($CDCl_3$): δ 8.70 (s, 2 H, phenyl), 3.47 (s, 1 H, CH); ^{13}C NMR ($CDCl_3$): δ 161.7, 160.1, 117.2, 85.6, 75.7; MS: *m/z* 138 (M^+). *Anal.* Calcd. for $C_6H_3ClN_2$ (138): C, 52.01; H, 2.18; N, 20.22; Found: C, 52.72; H, 2.14; N, 19.36%.

2-Methoxy-5-ethynylpyrimidine (2e). 6.0 g (4.9 mmol) 2-methoxy-5-(trimethylsilylethynyl)pyrimidine (**3e**) in 20 mL acetonitrile and 10 mL of the KOH solution was used. Purification by extraction with diethyl ether yielded 1.6 g (60%) of a white solid, mp 82°C, ^1H NMR ($CDCl_3$): δ 8.61 (s, 2 H, phenyl), 4.04 (s, 3 H, CH_3), 3.65 (s, 1 H, CH); ^{13}C NMR ($CDCl_3$): δ 164.2, 161.9, 161.2, 111.6, 82.2, 77.0, 55.2.

Synthesis of 1a–1e. The coupling procedure as described for preparation of **3a–3e** applies. Specific details for each compound are given in the following sections.

4,4′-Ethyn-1,2-diyl-bis-(2,6-dichloropyridine) (1a). 1.2 g (4.5 mmol) 2,6-dichloro-4-iodopyridine (**4a**), 0.8 g (4.7 mmol) 2,6-dichloro-4-ethynylpyridine (**2a**), and the catalyst in a mixture of 30 mL diisopropylamine and 30 mL tetrahydrofuran were used. After stirring for 4 h at room temperature, the reaction was complete. Purification by column chromatography (SiO_2; *n*-hexane/ethyl acetate; 20 : 1) yielded 0.8 g (56%) of a white solid, mp 140°C, IR: ArCH 3107, 3072, CC, NC 1575, 1521, CCl 1103 cm^{-1}; ^1H NMR ($CDCl_3$): δ 7.38 (s, 4 H, phenyl); ^{13}C NMR ($CDCl_3$): δ 151.2, 134.1, 124.7, 90.2; MS: *m/z* 318 (M^+); *Anal.* Calcd. for $C_{12}H_4Cl_4N_2$ (317.99): C, 45.33; H, 1.27; N, 8.81; Found: C, 45.55; H, 1.19; N, 8.64%.

5,5′-Ethyn-1,2-diyl-bis-(2-chloropyridine) (1b). 2.2 g (9.2 mmol) 2-chloro-5-iodopyridine (**4b**), 1.3 g (9.6 mmol) 2-chloro-5-ethynylpyridine (**2b**), and the catalyst in a mixture of 70 mL diisopropylamine and 60 mL tetrahydrofuran were used. After refluxing for 30 min, the reaction was complete. Purification by column chromatography (SiO_2; *n*-hexane/ethyl acetate; 1 : 1) yielded 1.5 g (67%) of a white solid, mp 230°C, IR: ArCH 3094, CN 1676, CC 1584, 1546, CCl 1017 cm^{-1}; ^1H NMR ($CDCl_3$): δ 8.56 (d, 2 H, ^4J = 2.1 Hz, phenyl), 7.77 (dd, 2 H, ^3J = 8.0 Hz, ^4J = 2.1 Hz, phenyl), 7.36 (d, 2 H, ^3J = 8.0 Hz, phenyl); ^{13}C NMR ($CDCl_3$): δ 152.1, 151.3, 140.9, 124.1, 118.3, 89.0; MS: *m/z* 249 ($M + H^+$); *Anal.* Calcd. for $C_{18}H_{22}N_4S_2$ (247.99): C, 57.86; H, 2.43; N, 11.25; Found: C, 57.99; H, 2.29; N, 11.16%.

5,5′-Ethyn-1,2-diyl-bis-[2-(t-butylthio)pyrimidine] (1c). 2.6 g (8.8 mmol) 2-(*t*-butylthio)-5-iodopyrimidine (**4c**), 1.8 g (9.1 mmol) 2-(*t*-butylthio)-5-ethynylpyrimidine (**2c**), and the catalyst in a mixture of 60 mL diisopropylamine and 60 mL tetrahydrofuran were used. After stirring for 90 min at room temperature, the reaction was complete. Purification by column chromatography (SiO_2; *n*-hexane/ethyl acetate; 1 : 20) yielded 2.4 g (77%) of a white solid, mp 57°C, IR: ArCH 2963, CN 1533, CH 1361 cm^{-1}; ^1H NMR ($CDCl_3$): δ 8.61 (s, 4 H, phenyl), 1.63 (s, 18 H, CH_3); ^{13}C NMR ($CDCl_3$): δ 172.7, 158.3, 113.1, 88.8, 48.0, 29.9; MS: *m/z* 359 ($M + H^+$); *Anal.* Calcd. for $C_{18}H_{22}N_4S_2$ (358.13): C, 60.30; H, 6.18; N, 15.63; S, 17.89; Found: C, 60.38; H, 6.32; N, 15.62; S, 17.90%.

5,5′-Ethyn-1,2-diyl-bis-(2-chloropyrimidine) (1d). 1.9 g (8.0 mmol) 2-chloro-5-iodopyrimidine (**4d**), 1.3 g (9.4 mmol) 2-chloro-5-ethynylpyrimidine (**2d**), and the catalyst in a mixture of 60 mL diisopropylamine and 60 mL tetrahydrofuran were used. After refluxing for 8 h, the reaction was complete. Purification by column chromatography (SiO_2; *n*-hexane/ethyl acetate; 2 : 1) yielded 1.4 g (61%) of a yellow solid, mp 205°C, IR: ArCH 3037, CN 1730, CC 1587, 1527, CCl 1036 cm^{-1}; ^1H NMR (DMSO-d_6): δ 8.87 (s, 4 H, phenyl); ^{13}C NMR (DMSO-d_6): δ 160.1, 158.7, 115.7, 87.8; MS: *m/z* 249 ($M + H^+$); *Anal.* Calcd. for $C_{10}H_4Cl_2N_4$ (249.98): C, 47.84; H, 1.61; N, 22.32; Found: C, 48.24; H, 1.60; N, 21.90%.

5,5′-Ethyn-1,2-diyl-bis-(2-methoxypyrimidine) (1e). 1.7 g (7.0 mmol) 5-iodo-2-methoxypyrimidine (**4e**), 1.0 g (7.5 mmol) 2-methoxy-5-ethynylpyrimidine (**2e**), and the catalyst in a mixture of 75 mL of diisopropylamine and 75 ml tetrahydrofuran were used. After refluxing for 30 min, the reaction was complete. Purification by column chromatography (SiO_2; *n*-hexane/ethyl acetate; 2 : 1) yielded 1.2 g (70%) of a white solid, mp 182°C, IR: ArCH 3015, 2993, CH 2942, CC 1597, 1530, CO 1287 cm^{-1}; ^1H NMR ($CDCl_3$): δ 8.67 (s, 4 H, phenyl), 4.07 (s, 3 H, CH_3); ^{13}C NMR ($CDCl_3$): δ 164.2, 161.1, 111.9, 87.2, 55.2; ms: *m/z* 242 (M^+); *Anal.* Calcd. for $C_{12}H_{10}N_4O_2$ (242.08): C, 59.50; H, 4.16; N, 23.13; Found: C, 59.47; H, 3.88; N, 22.83%.

X-ray structure determination. Crystals suitable for single-crystal X-ray diffraction studies were obtained by slow cooling of solutions of the respective compounds in chloroform. Information concerning the crystallographic data and the refinement calculations of the two compounds is summarized in Table 1. The intensity data were collected on a Bruker APEX II diffractometer with MoKα radiation (λ = 0.71073 Å) using ω and φ scans. Intensities were corrected for background, Lorentz, and polarization effects. Preliminary structure models were derived by an application of direct methods [47] and were refined by full matrix least-squares calculations based on F^2 for all reflections [48]. All non-hydrogen atoms were refined anisotropically. All hydrogen atoms were included in the models in calculated positions and were refined as constrained to bonding atoms.

CCDC 947220 (**1a**), 947221 (**1b**), 947222 (**1c**), 947223 (**1d**), and 947224 (**1e**) contain the supplementary crystallographic data for this article. These data can be obtained free of charge from the Cambridge Data Centre *via* www.ccdc.cam.ac.uk/data_request/cif.

Acknowledgment. This work was performed within the Cluster of Excellence "Structure Design of Novel High-Performance Materials *via* Atomic Design and Defect Engineering (ADDE)," which is financially supported by the European Union (European Regional Development Fund) and by the Ministry of Science and Art of Saxony (SMWK).

REFERENCES AND NOTES

[1] Health, E.; Kosjek, T. Topics in Heterocyclic Chemistry; Iskra, J. Ed.; Springer: Berlin, Heidelberg, 2012, pp 219–246.

[2] Schirok, H.; Paulsen, H.; Kroh, W.; Chen, G.; Gao, P. Org Process Res Dev 2010, 14, 168.

[3] Venturoni, F.; Nikbin, N.; Ley, S. V.; Baxendale, I. R. Org Biomol Chem 2010, 8, 1798.

[4] Sillion, B. High Perform Polym 1999, 11, 417.

[5] Baker, R.; Jones, C. Coord Chem Rev 2005, 249, 1857.

[6] Curtis, N. F. In Comprehensive Coordination Chemistry II; McCleverty, J. A.; Meyer, T. J. Ed.; Elsevier: Amsterdam, 2003, pp 447–474.
[7] Smith, A. P.; Fraser, C. L. In Comprehensive Coordination Chemistry II; McCleverty, J. A.; Meyer, T. J. Ed.; Elsevier: Amsterdam, 2003, pp 1–23.
[8] Bai, S.-Q.; Young, D. J.; Hor, T. S. Andy Chem Asian J 2011, 6, 292.
[9] Van Leeuwen, P. W. N. M. Supramolecular Catalysis; Wiley-VCH: Weinheim, 2008, pp 57–86.
[10] Uehara, K.; Kasai, K.; Mizuno, N. Inorg Chem 2010, 49, 2008.
[11] Matouzenko, G. S.; Jeanneau, E.; Verat, A. Y.; de Gaetano, Y. Eur J Inorg Chem 2012, 969.
[12] Winter, S.; Weber, E.; Eriksson, L.; Csöregh, I. New J Chem 2006, 30, 1808.
[13] Bosch, E.; Barnes, C. L. New J Chem 2001, 25, 1376.
[14] Bosch, E.; Barnes, C. L. J Coord Chem 2005, 58, 1021.
[15] Georgiev, I.; Barnes, C. L.; Bosch, E. J Supramol Chem 2001, 1, 153.
[16] Schindler, D.; Eißmann, F.; Weber, E. Org Biomol Chem 2009, 7, 3549.
[17] Georgiev, I.; Bosch, E.; Barnes, C. L.; Draganjac, M. Cryst Growth Des 2004, 4, 235.
[18] Baxter, P. N. W. J Org Chem 2000, 65, 1257.
[19] Schlosser, M.; Bobbio, C.; Rausis, T. J Org Chem 2005, 70, 2494.
[20] Edgar, K. J.; Falling, S. N. J Org Chem 1990, 55, 5287.
[21] Schaetzer, J.; Wenger, J.; Berteina-Raboin, S.; Stoller, A.; Nebel, K.; Hall, R. G. European Patent, WO2003050087, 2003.
[22] Pérez-Balado, C.; Ormerod, D.; Aelterman, W.; Mertens, N. Org Process Res Dev 2007, 11, 237.
[23] Efange, S.; Cheng, Y.-C.; Bardos, T. Nucleos Nucleot Nucl 1985, 4, 545.
[24] Sonogashira, K.; Tohda, Y.; Hagihara, N. Tetrahedron Lett 1975, 16, 4467.
[25] Desiraju, G. R.; Steiner, T. The Weak Hydrogen Bond: In Structural Chemistry and Biology; Oxford University Press: Oxford, 1999.
[26] Cook, E. G. J Chem Phys 1970, 53, 723.
[27] Steed, J. W.; Atwood, J. L. Supramolecular Chemistry; Wiley: Chichester, UK, 2009, pp 33–35.
[28] Desiraju, G. R. Crystal Engineering: The Design of Organic Solids; Elsevier: Amsterdam, 1989.
[29] Sokolov, A. N.; Friščić, T.; Blais, S.; Ripmeester, J. A.; MacGillivray, L. R. Cryst Growth Des 2006, 6, 2427.
[30] Bosch, E. Cryst Growth Des 2010, 10, 3808.
[31] Giannozzi, P. et al. J Phys Condens Matter 2009, 21, 395502.
[32] Hu, F.; Guan, X.; Shi, M. Tetrahedron 2012, 68, 4782.
[33] Banerjee, R.; Phan, A.; Wang, B.; Knobler, C.; Furukawa, H.; O'Keeffe, M.; Yaghi, O. M. Science 2008, 319, 939.
[34] Ye, C.; Gao, H.; Boatz, J. A.; Drake, G. W.; Twamley, B.; Shreeve, J. M. Angew Chem Int Ed 2006, 45, 7262.
[35] Brammer, L.; Bruton, E. A.; Sherwood, P. Cryst Growth Des 2001, 1, 277.
[36] Cozzi, F.; Annunziata, R.; Benaglia, M.; Cinquini, M.; Raimondi, L.; Baldridge, K. K.; Siegel, J. S. Org Biomol Chem 2003, 1, 157.
[37] Georgiev, I.; Bosch, E.; Barnes, C. L. J Chem Crystallogr 2004, 34, 859.
[38] Taylor, R.; Kennard, O. J Am Chem Soc 1982, 104, 5063.
[39] Pedireddi, V. R.; Shekhar Reddy, D.; Satish Goud, B.; Craig, D. C.; David Rae, A.; Desiraju, G. R. J Chem Soc, Perkin Trans 1994, 2, 2353.
[40] Zhang, J.-G.; Ruan, L.-L.; Zhao, J.-H.; Zhu, G.-N. Chin J Struct Chem 2011, 30, 1132.
[41] Ma, M.; Wang, H.; Li, X.; Liu, L.; Jin, H.; Wen, K. Tetrahedron 2009, 65, 300.
[42] Wang, Q.-Q.; Wang, D.-X.; Yang, H. B.; Huang, Z.-T.; Wang, M.-X. Chem-Eur J 2010, 16, 7265.
[43] Jarzembska, K. N.; Kubsik, M.; Kamiński, R.; Woźniak, K.; Dominiak, P. M. Cryst Growth Des 2012, 12, 2508.
[44] Kitaigorodskii, A. L. Molecular Crystals and Molecules; Academic Press: New York, 1973.
[45] Räth, C. Justus Liebigs Ann Chem 1931, 486, 71.
[46] Arantz, B. W.; Brown, D. J. J Chem Soc C 1971, 1889.
[47] Sheldrick, G. M. Acta Cryst 1990, A46, 467.
[48] Sheldrick, G. M. Acta Cryst 2008, A64, 112.
[49] Perdew, J. P.; Burke, K.; Ernzerhof, M. Phys Rev Lett 1996, 77, 3865.